



Published in final edited form as:

*Genes Chromosomes Cancer*. 2010 March ; 49(3): 224–236. doi:10.1002/gcc.20731.

## Recurrent (2;2) and (2;8) Translocations in Rhabdomyosarcoma without the Canonical *PAX-FOXO1* fuse *PAX3* to Members of the Nuclear Receptor Transcriptional Coactivator (*NCOA*) Family

Janos Sumegi<sup>1</sup>, Renae Streblov<sup>2</sup>, Robert W. Frayer<sup>1</sup>, Paola Dal Cin<sup>3</sup>, Andrew Rosenberg<sup>4</sup>, Aurelia Meloni-Ehrig<sup>5</sup>, and Julia A. Bridge<sup>2,6,7,\*</sup>

<sup>1</sup>Division of Hematology/Oncology, Cincinnati Children's Hospital Medical Center, University of Cincinnati, Faculty of Medicine, Cincinnati, OH

<sup>2</sup>Departments of Pathology and Microbiology, University of Nebraska Medical Center, Omaha, NE

<sup>3</sup>Department of Pathology, Harvard Medical School, Boston, MA

<sup>4</sup>Department of Pathology, Massachusetts General Hospital, Boston, MA

<sup>5</sup>Department of Cytogenetics, Quest Diagnostics Nichols Institute, Chantilly, VA

<sup>6</sup>Department of Pediatrics/Meyer Munroe Institute, University of Nebraska Medical Center, Omaha, NE

<sup>7</sup>Department of Orthopaedic Surgery, University of Nebraska Medical Center, Omaha, NE

### Abstract

The fusion oncoproteins *PAX3-FOXO1* [t(2;13)(q35;q14)] and *PAX7-FOXO1* [t(1;13)(p36;q14)] typify alveolar rhabdomyosarcoma (ARMS); however, 20-30% of cases lack these specific translocations. In this study, cytogenetic and/or molecular characterization to include FISH, RT-PCR and sequencing analyses of five rhabdomyosarcomas [four ARMS and one embryonal rhabdomyosarcoma (ERMS)] with novel, recurrent t(2;2)(p23;q35) or t(2;8)(q35;q13) revealed that these non-canonical translocations fuse *PAX3* to *NCOA1* or *NCOA2* respectively. The *PAX3-NCOA1* and *PAX3-NCOA2* transcripts encode chimeric proteins composed of the paired-box and homeodomain DNA-binding domains of *PAX3*, and the CID domain, the Q-rich region and the AD2 domain of *NCOA1* or *NCOA2*. To investigate the biological function of these recurrent variant translocations, the coding regions of *PAX3-NCOA1* and *PAX3-NCOA2* cDNA constructs were introduced into expression vectors with tetracycline-regulated expression. Both fusion proteins showed transforming activity in the soft agar assay. Deletion of the AD2 portion of the *PAX3-NCOA* fusion proteins reduced the transforming activity of each chimeric protein. Similarly, but with greater impact, CID domain deletion fully abrogated the transforming activity of the chimeric protein. These studies: (1) expand our knowledge of *PAX3* variant translocations in RMS with identification of a novel *PAX3-NCOA2* fusion; (2) show that both *PAX3-NCOA1* and *PAX3-NCOA2* represent recurrent RMS rearrangements; (3) confirm the transforming activity of both translocation events and demonstrate the essentiality of intact AD2 and CID domains for optimal transforming activity; and, (5) provide alternative approaches (FISH and RT-PCR) for detecting *PAX-NCOA* fusions in nondividing cells of RMS. The latter could potentially be utilized as aids in diagnostically challenging cases.

\*Correspondence to: Julia A. Bridge, M.D., FACMG Department of Pathology and Microbiology 983135 Nebraska Medical Center Omaha, NE 68198-3135 Phone: 402-559-7212 Fax: 402-559-6018 jbridge@unmc.edu.

## INTRODUCTION

Rhabdomyosarcomas are the largest subset of soft tissue sarcomas in infants and children and are highly heterogeneous, clinically aggressive tumors that show varying degrees of skeletal muscle differentiation (Raney et al., 2001). The two main histological patterns recognized include embryonal rhabdomyosarcoma (ERMS) and alveolar rhabdomyosarcoma (ARMS). Morphologic evaluation alone is often insufficient to make the distinction between ARMS and ERMS as some ARMS lack the alveolar architecture (“solid variant”) and ERMS can be densely cellular and poorly differentiated (Parham et al., 2006). This distinction is clinically critical however, in assigning patients appropriately to high-risk therapeutic regimens. Thus, a valuable diagnostic adjunct in ARMS is the identification of translocations  $t(2;13)(q35;q14)$  and  $t(1;13)(p36;q14)$ , and the associated *PAX3-FOXO1* and *PAX7-FOXO1* fusion transcripts, respectively. Recognition of these specific translocations is also prognostically important as *PAX3-FOXO1* positive ARMSs are significantly more aggressive than *PAX7-FOXO1* ARMSs (Sorensen et al., 2002).

The vast majority of ARMSs exhibit *PAX-FOXO1* fusion transcripts that encode for proteins composed of a *PAX* paired domain and homeodomain DNA-binding element (NH<sub>2</sub>-terminus) and a *FOXO1* transactivation domain (COOH-terminus) (Galili et al., 1993; Davis et al., 1994). The *PAX-FOXO1* chimeric products are highly expressed in the tumor cells, exclusively localized in the nucleus, and are more potent transcriptional activators than wild type *PAX3*, *PAX7* or *FOXO1*. Approximately 30% of ARMSs fail to exhibit either *PAX3-FOXO1* or *PAX7-FOXO1* fusions by routine RT-PCR and have been termed “fusion transcript negative” (Barr et al., 2002). Rare, isolated cases have shown alternate translocation associated fusion transcripts (*PAX3-AFX* and *PAX3-NCOA1*) (Barr et al., 2002; Wachtel et al., 2004). In the current study, a novel genetic subgroup of rhabdomyosarcoma with recurrent chromosomal translocations fusing *PAX3* to members of the nuclear receptor coactivator family of genes to include *NCOA1* [ $t(2;2)(p23;q35)$ ] or *NCOA2* [ $t(2;8)(q35;q13)$ ] in lieu of a forkhead domain family member was identified and characterized.

## MATERIALS AND METHODS

### Tumor Samples

Five rhabdomyosarcoma specimens that were determined to be negative for a rearrangement of the *FOXO1* locus by FISH or a *PAX3*- or *PAX7-FOXO1* fusion transcript by RT-PCR were included in the study. The clinicohistopathologic features of the patients and corresponding tumors are listed in Table 1. The histopathological diagnoses were established in accordance with the International Classification of Rhabdomyosarcoma criteria (Qualman et al., 1998). Histologic and immunohistochemical features typical of ARMS and ERMS were identified in the respective cases (Fig. 1). No distinctive clinical phenotype was recognized that might distinguish these *PAX-NCOA* fusion positive cases from other alveolar or embryonal rhabdomyosarcomas. The karyotype of one patient has been reported previously (case 5) (Meloni-Ehrig et al., 2009).

### Cytogenetic Analysis

Cytogenetic analysis was performed on sterile representative samples of cases 2, 4, and 5 using standard culture and harvesting procedures (Bridge et al., 2000). Metaphase cells were banded with Giemsa trypsin, and the karyotypes were described according to the International System for Human Cytogenetic Nomenclature 2009 (ISCN, 2009).

## Probe Design and Development

Bacterial artificial chromosome (BAC) and yeast artificial chromosome (YAC) clones for the *PAX3*, *NCOA1*, and *NCOA2* gene regions were identified utilizing the NCBI Map Viewer (<http://www.ncbi.nlm.nih.gov/mapview>), the Ensembl Genome Browser (<http://www.ensembl.org>), the University of California Santa Cruz (UCSC) Human Genome Browser Gateway (<http://genome.ucsc.edu/cgi-bin/hgGateway>), and the Whitehead Institute/MIT Center Genome Browser ([http://www-genome.wi.mit.edu/cgi-bin/contig/yac\\_info](http://www-genome.wi.mit.edu/cgi-bin/contig/yac_info)). The *PAX3* probe sets utilized have been previously described (Nishio et al., 2006). Combinations of probe sets were custom-designed to flank and span *NCOA1* and *NCOA2* (Table 2).

## Fluorescence In Situ Hybridization

Two-color FISH studies were performed on cytologic touch preparations ( $n = 2$ ), in situ metaphase cell preparations ( $n = 1$ ), and formalin-fixed, paraffin-embedded tissue sections ( $n = 3$ ). Probes were directly labeled by nick translation with either Spectrum Green or Spectrum Orange-dUTP utilizing a modification of the manufacturer's protocol (Abbott Molecular Inc., Des Plaines, IL, USA) (Nishio et al., 2006; Kapels et al., 2007).

Prior to hybridization, the touch preparations and in situ slides were pretreated as previously described (Nishio et al., 2006). Following pretreatment, the cells and probes were codenatured at 75°C for 1-6 min and incubated at 37°C overnight using the HYBrite™ denaturation/hybridization system (Nishio et al., 2006; Kapels et al., 2007). Post-hybridization washing was performed in 0.4x SSC/0.3% NP-40 at 72°C for 2 min, followed by 2x SSC/0.1% NP-40 at room temperature for 1 min. The slides were air-dried in the dark and counterstained with 10µl of 4',6-diamidino-2-phenylindole (DAPI II; Abbott Molecular). Hybridization signals were assessed in 200 interphase nuclei with strong and well-delineated signals by two different individuals. An interphase cell specimen was interpreted as abnormal if spanning probe signals for the *NCOA1* or *NCOA2* genes fused with the spanning probe signal for the *PAX3* gene, or if a split of flanking probe signals (defined as more than a signal size apart) was detected in more than 10% of the cells evaluated (more than two standard deviations above the average false-positive rate). Negative controls included normal peripheral blood lymphocytes and cytologic touch preparations of pathologically unremarkable skeletal muscle. Images were acquired by use of the CytoVision Image Analysis System (Applied Imaging, Santa Clara, CA, USA).

## Identification of *PAX3-NCOA1* and *PAX3-NCOA2* Fusion Transcripts

Total RNA was isolated using the RNeasy Mini Kit (Qiagen, Valencia, CA). The 3'-RACE (3'-rapid amplification of cDNA ends) was performed using the SMART-RACE cDNA amplification kit and protocol (Clontech, Palo Alto, CA). Briefly, first-strand cDNA was reverse transcribed from 0.5 µg total RNA using Superscript II and the 3'-RACE cDNA synthesis primer (3'-CDS) from the kit. An aliquot of the first-strand cDNA was then amplified using a *PAX3* gene-specific forward primer (PAX3-32, Table 3) and a universal primer mix (SMART-RACE kit). Polymerase chain reaction (PCR) conditions were as recommended by the manufacturer. A nested PCR reaction using the nested universal primer (SMART-RACE kit) as the reverse primer and PAX3-34 (internal to PAX3-32, Table 3) as the forward primer was performed according to the manufacturer's instructions. Second-round PCR products were electrophoresed, purified, and subcloned into *E. coli* OneShot® competent cells (Invitrogen, Carlsbad, CA). Plasmid DNAs were purified, analyzed for the presence of insert by restriction enzyme digestion and sequenced.

### RT-PCR for *PAX3-NCOA1* and *PAX3-NCOA2*

First-strand cDNA was reverse transcribed from 0.5µg of total RNA with the Advantage RT-PCR System with random or oligo(dT) primers (Clontech). For the detection of a *PAX3-NCOA1* fusion transcript, RT-PCR was conducted with a forward primer (PAX3-32, Table 3) specific for exon 6 of *PAX3* and reverse primers (NCOA1-33 and NCOA1-35, Table 3) specific for different exons of *NCOA1*. Similarly, RT-PCR was used to detect *PAX3-NCOA2* fusion transcripts, with *PAX3* specific forward primers (PAX3-41, -45, Table 3) and *NCOA2* specific reverse primers (NCOA2-44; -48, Table 3) the amplification products were cloned in pCR4/TOPO (Invitrogen), sequenced, and analyzed using MacVector Version 10 (MacVector Inc. Cary, NC).

### Construction of Full Length *PAX3-NCOA1* and *PAX3-NCOA2* cDNA

Full length *PAX3-NCOA1* and *PAX3-NCOA2* cDNAs were constructed using cloned cDNA fragments obtained from the RT-PCR and RACE assays and inserted in pCR4-TOPO. The full length cDNA of *PAX3-NCOA1* and *PAX3-NCOA2* was assembled by PCR-based gene synthesis using a 2-step assembly/amplification protocol (Carr et al., 2004) with the exception that the assembly PCR was run for 45 cycles. The primary structure of the constructs was confirmed by nucleotide sequence analysis using pCR4 and gene specific sequencing primers.

### Construction of Tetracycline Inducible, *PAX3-NCOA1* or *PAX3-NCOA2* Mammalian Expression Vectors

The coding region of *PAX3-NCOA1* and *PAX3-NCOA2* fusion constructs was PCR amplified using pCR4-TOPO cloned *PAX3-NCOA1* and *PAX3-NCOA2* with the Expand High Fidelity PCR System (Roche Diagnostics, Indianapolis, IN) in the presence of gene specific primers (Table 3). The amplified coding regions were introduced into the tetracycline inducible mammalian expression vector pcDNA4/TO, after sequencing two clones were selected; pcDNA4-PAX33-NCOA1.23 and pcDNA4-PAX3-NCOA2.1.

To establish the tetracycline-regulated system, NIH3T3 cells were first stably transfected using Effectene Transfection Reagent (Qiagen) with pcDNA6/TR (Invitrogen, Carlsbad, CA), which encodes the Tet repressor (TeR) under the control of human CMV promoter. Subsequently, clones were selected and maintained in tetracycline-free medium (Clontech) containing 5 µg/mL Blasticidin (Invitrogen). The inducibility of each clone was tested by transient transfection with pcDNA4/TO/LacZ and stained for β-gal (Invitrogen). The clone (NIH 3T3-Tet-19.1) demonstrating the highest LacZ induction was selected for generating a stable cell line with tetracycline regulated *PAX3-NCOA1* or *PAX3-NCOA2* expression.

### Construction of *PAX3-NCOA1* or *PAX3-NCOA2* Deletion Mutants

*PAX3-NCOA1* or *PAX3-NCOA2* deletion mutants in pcDNA4/TO were created using two consecutive steps to delete either AD1 or AD2 regions of *NCOA1* and *NCOA2* utilizing the QuickChange kit (Stratagene, La Jolla, CA) with primers listed in Table 4.

### Sequence Analysis

Plasmid clones were sequenced using ABI PRISM® BigDye™ Terminator Cycle Sequencing Kit version 2 and ABI PRISM® 3730 DNA Analyzer, a capillary electrophoresis system (ABI). Sequence analysis was performed using the MacVector with Assembler Version 10.0.2 (MacVector, Inc. Cary, NC) sequence analysis program.

### Tetracycline Regulated Expression

The expression constructs pcDNA4-PAX33-NCOA1.23 and pcDNA4-PAX3-NCOA2.1 were transfected into NIH3T3-Tet-19.1 and selected on 500- $\mu$ g/ml zeocin for 7 - 10 days. Tetracycline-free medium containing 5  $\mu$ g/mL Blastidicin (Invitrogen) and 400  $\mu$ g/mL Zeocin (Invitrogen) was used for maintaining the transfected cells. Induction of pcDNA4-PAX3/NCOA1 and pcDNA4/TO-PAX3/NCOA2 and deletion mutants was accomplished by adding 1  $\mu$ g/ml tetracycline to media and tested by reverse transcription-PCR (RT-PCR) and Western blot.

### Growth of Cells in Semi-solid Media

Transformation of NIH3T3 cells by *PAX3*, *PAX3-FOXO1*, and their variants was examined using a colony formation in soft agar culture assay. Following selection, 4000 cells were embedded in soft agar as described by Lugo and Witte (1989) and were seeded in six well plates in culture medium (DMEM/F12) 14-21 days with fresh medium supplementation every 3 days before colonies were counted and photographed. Colonies larger than 100 mm were counted for each plate. Experiments were repeated three times with duplicate plates for each cell line.

### Western Analyses and Immunoblotting

To verify the anticipated expression of the various constructs, the constructs were transfected into NIH 3T319.1 cells and expression of the cloned genes was induced by tetracycline (1  $\mu$ g/ml). For detecting in vitro expression of PAX3-NCOA1 and PAX3-NCOA2 and their derivatives, confluent cells were rinsed with cold phosphate-buffered saline twice and lysed in the presence M-PER (Pierce, Thermo Fisher Scientific Inc. Rockford, IL). Whole cell lysates were fractionated on precasted 4-15% SDS-polyacrylamide gels (BioRad) and analyzed by Western blot. The expression of PAX3-NCOA1 and PAX3-NCOA2 or their derivatives was detected by the primary PAX3 antibody (N19, sc-7749, Santa Cruz Biotechnology, Inc. Santa Cruz CA). The secondary anti-rabbit IgG antibody was used at a dilution of 1:3000. To confirm that equal amounts of protein extract were loaded, the level of  $\beta$ -actin levels in the cell lysate were assessed using anti- $\beta$ -actin (sc-81178) with secondary antibodies anti-goat IgG (sc-2378) and anti-mouse IgG (sc-2005), (Santa Cruz Biotechnology, Inc). Immune complexes were detected by chemiluminescence using SuperSignal reagents (Thermo Scientific, Rockford, IL).

## RESULTS

### Cytogenetic Analysis

Cytogenetic analysis conducted on cases 2, 4, and 5 revealed the presence of a balanced 2;8 translocation involving 2q35 and a near identical 8q breakpoint (q12-13) in cases 4 and 5 (Fig. 2). An abnormal clone was not identified in case 2.

### Fluorescence In Situ Hybridization

All cases exhibited a rearrangement of the *PAX3* gene locus using the custom-designed breakpoint flanking probe set. Subsequent analysis with the custom-designed *NCOA1* and *NCOA2* breakpoint flanking and spanning probe sets confirmed the presence of a rearrangement of *NCOA1* and fusion with *PAX3* (*PAX3-NCOA1*) in cases 1, 2 and 3, and a rearrangement of *NCOA2* and fusion with *PAX3* (*PAX3-NCOA2*) in cases 4 and 5 (Fig. 3).

### Characterization of the *PAX3-NCOA1* and *PAX3-NCOA2* Translocations

Sequence analysis of the *PAX3* 3'-RACE PCR products of case 2 revealed fusion of the first 7 exons of *PAX3* to the last 10 exons of the nuclear receptor coactivator gene *NCOA1*.



Subsequent RT-PCR analysis with *PAX3* forward and *NCOA1* reverse primers of this case and case 3 showed that the fusion cDNA junctions for *PAX3-NCOA1* were identical (fusion of exon 7 of *PAX3* with exon 11 of *NCOA1*) (Figs. 4 and 5). In contrast, RT-PCR analysis of the ARMS specimen of case 1 revealed a gel electrophoresis amplification product that was slightly smaller in size than the products of cases 2 and 3 (Fig. 4). Consequent sequence analysis of this smaller product demonstrated an in-frame fusion of *PAX3* exon 6 with *NCOA1* exon 12, a *PAX3-NCOA1* fusion transcript similar to that described by Wachtel et al., (2004) (Figs. 4 and 5).

The *PAX3-NCOA1* fusion protein of case 1 is composed of the DNA-binding domains of *PAX3* (paired-box and homeodomain; 319 N-terminal AA) and the C-terminal region of *NCOA1* presumably functioning as a transactivation domain (includes the CID/AD1 domain, the Q-rich region and the AD2 domain covering 575 AA), (Fig. 5). The resulting chimeric protein (1,026 residues in total) for cases 2 and 3 includes the initial 391 AA of *PAX3* joined to the C-terminal 635 AA of *NCOA1* (Fig. 5). Both DNA-binding domains of *PAX3* (paired-box and homeodomain) and the interaction domain (CID/AD1), the Q-rich region and the transactivation domain 2 (AD2) of *NCOA1* are incorporated into the fusion protein (Fig. 5). We refer to the *PAX3-NCOA1* chimeric protein in case 1 as a type 1 fusion and the chimeric proteins of cases 2 and 3 as a type 2 fusion.

Cloning and sequencing of the RACE-PCR products of case 4 revealed that exon 7 of *PAX3* was fused to exon 12 of the *NCOA2* gene, the second member of the nuclear receptor transcriptional coactivator family of genes (Figs. 4 and 6). Subsequent RT-PCR analysis with *PAX3* forward and *NCOA2* reverse primers of this case and case 5 which also exhibited a 2;8 translocation karyotypically, showed identical *PAX3-NCOA2* fusion breakpoints (Fig. 6). Reciprocal *NCOA2-PAX3* transcripts were not detected. The full-length cDNA construct extended 4,724 nucleotides of which 3,171 are coding. The resulting *PAX3-NCOA2* fusion protein is 1057 AA long and consists of the 391 N-terminal AA of *PAX3* (DNA-binding domains) and the 666 C-terminal AA of *NCOA2* (CID/AD1 domain, the Q-rich region and the AD2 domain 2), (Fig. 6).

In an effort to examine the oncogenic consequences of *PAX3-NCOA1* type 1, *PAX3-NCOA1* type 2, and *PAX3-NCOA2* expression, a cell culture system using a tetracycline regulated mammalian expression system (T-REx™ system, Invitrogen) was employed. In this model system, NIH 3T3 cells were transfected with pcDNA6/TR plasmid expressing the *tet* repressor. Following transfection several clones expressing the *tet* repressor were selected. NIH 3T3-19.1 was preferred due its high inducibility by addition of tetracycline and low leakage in the absence of the drug and was used for the subsequent experiments. *PAX3-NCOA1* type 1, *PAX3-NCOA1* type 2, and *PAX3-NCOA2* fusion transcripts were cloned into pcDNA4/TO vector and transfected into NIH-3T3-19.1 cells. After transduction into NIH-3T3-19.1 cells and selection in zeocin, Western blotting demonstrated that the expression level of *PAX3-NCOA1* type 1, *PAX3-NCOA1* type 2, and *PAX3-NCOA2* chimeric genes was regulated by the concentration of tetracycline in the medium (Fig. 7A). Western blotting analysis revealed a rapid induction of *PAX3-NCOA1* type 1 proteins as early as 4 hours and reached the peak level at 36 hours (Fig. 7B).

### Transforming Properties of *PAX3-NCOA1* and *PAX3-NCOA2*

Zeocin resistant polyclonal cells from *PAX3-NCOA1* type 1, *PAX3-NCOA1* type 2 and *PAX3-NCOA2* transfectants were assayed in the presence of 1 µg/ml tetracycline for anchorage independent growth in liquid medium and colony formation in soft agar (Fig. 8). Cells expressing *NCOA1* or *NCOA2* showed anchorage independent growth (Fig. 8A) and displayed macroscopically visible colonies in soft agar (Fig. 8B). In contrast cells

transfected with the empty vector showed no visible colony formation and displayed a flat morphology when grown on plastic (Fig. 8A).

The CID/AD1 domain of NCOA proteins is important to recruit CBP/p300 into the nuclear receptor mediated transcriptional complex to acetylate histone and non-histone proteins and to promote transcription (Voegel et al., 1996; Li et al., 1997; Onate et al., 1998). The second transcriptional activation domain (AD2), also located at the C terminus of NCOA proteins, is responsible for interaction with histone methyltransferases, coactivator-associated arginine methyltransferase-1 and protein arginine methyltransferase 1 (Chen et al., 1999; Koh et al., 2001). Both CID/AD1 and AD2 are important functional domains and both are retained in the PAX3-NCOA1 and PAX3-NCOA2 fusion proteins.

To explore the involvement of the CID/AD1 and AD2 domains in the oncogenic activity of *PAX3-NCOA1* and *PAX3-NCOA2*, targeted deletions were introduced. The AD1 and AD2 deletions represent in-frame deletions from Ser357 to Gly411 (CID, AD1 domain) and from Ser697 to Pro727 (AD2 domain) of the PAX3-NCOA1 type 1 protein. Corresponding deletions in PAX3-NCOA1 type 2 proteins were from Ser495 to Gly549 (AD1 /CID domain) and from Ser835 to Pro865 (AD2 domain) (Fig. 9A). The in-frame deletions in PAX3-NCOA2 were between Phe649 and Gly739 (CID/AD1 domain) and Val898 and Met931 (AD2 domain). Western blotting analysis verified the sizes and expression of the mutated proteins in NIH 3T3-19.1 cells (Fig. 9B).

NIH 3T3-Tet-19.1 cells transduced with the *PAX3-NCOA1* or *PAX3-NCOA2* lacking the AD2 domain result in decreased number of soft agar colonies (Fig. 9C). The deletion of CID/AD1 domain showed dramatic decrease in their ability to form colonies in soft agar suggesting (Fig. 9C) that the integrity of this region is important in oncogenic activity of the chimeric protein.

## DISCUSSION

At least 70% of alveolar rhabdomyosarcomas are characterized by the expression of one of two chimeric proteins generated by translocations that fuse the *FOXO1* gene with the *PAX3* or *PAX7* gene; the remainder of cases lack these translocations (fusion transcript negative ARMS). Following the design of novel *PAX3*, *PAX7* and *FOXO1* FISH probe sets, we uncovered a *PAX3* rearrangement in an ARMS case negative for *PAX3-FOXO1* and *PAX7-FOXO1* fusion transcripts (Nishio et al., 2006). This finding, suggesting the presence of a *PAX3* variant translocation, prompted an investigation of the potential translocation gene partner in this case and three additional fusion transcript negative ARMSs and one congenital ERMS, each also suspicious for containing *PAX3* variant translocations based on conventional cytogenetic and/or *PAX3* FISH analysis. Newly recurrent chimeric genes, as well as novel ones characterized by fusion of the *PAX3* gene with either *NCOA1* or *NCOA2* were identified in each case. *PAX3-NCOA1* is structurally heterogeneous and two types of in-frame *PAX3-NCOA1* chimeric transcripts were discovered. We have defined a “type 1” *PAX3-NCOA1* fusion transcript as one with the fusion breakpoint located in intron 6 of *PAX3* and in intron 12 of *NCOA1*; a rearrangement that has also been observed in an isolated case reported by Wachtel et al. (2004) among a series of 29 RMSs subjected to gene expression profiling. The designation “type 2” *PAX3-NCOA1* chimeric transcript is proposed for fusion of *PAX3* exon 7 with *NCOA1* exon 11.

The clinicohistopathologic findings of Case 5 were consistent with the diagnosis of congenital ERMS (Meloni-Ehrig et al., 2009). In contrast to ARMS, ERMS has not been classified as a translocation sarcoma. Rather, ERMSs frequently exhibit a recurrent pattern of chromosomal imbalances (gain of all or portions of chromosomes 2, 7, 8, 11, 12, 13 and/

or 20, with or without loss of 22) (Polito et al., 1999; Bridge et al., 2000). To the best of our knowledge, this is the third reported case of ERMS with cytogenetic abnormalities involving chromosomal breakpoints 2q35 and 8q13 (Hayashi et al., 1988; Yoshino et al., 2005). Recently, Davicioni et al. (2009) described a genomic-based classification scheme that is at variance with conventional histopathological schemes. Specifically, the gene expression profiles and LOH patterns of *PAX-FOXO1* negative ARMSs were indistinguishable from conventional ERMSs and thus, the authors concluded that RMS can be effectively divided into two main molecular classes (*PAX-FOXO1* positive and negative RMS). Moreover, it was proposed that it may be more appropriate to define tumors both by histological appearance (alveolar, embryonal, and the embryonal variants) and by fusion status (*PAX-FOXO1* positive and negative). This is an interesting concept as it relates to the presence of *PAX3* variant translocations, a genotype historically linked with an alveolar phenotype, in cases of histologic ERMS.

In contrast to *FOXO1*, *NCOA1* and *NCOA2* do not encode for transcriptional factors. *NCOA1* and *NCOA2*, in addition to *NCOA3* (20q13.12), are members of the p160 nuclear receptor transcriptional coactivator family. The proteins encoded by these genes have an overall sequence similarity of 50–55% between the three members (Xu and O'Malley, 2002; Xu and Li, 2003). Their most conserved N-terminal bHLH/PAS receptor nuclear translocator domain is involved in DNA binding and heterodimerization between proteins containing the same motifs. The intrinsic transcriptional activation domain, CID/AD1 is responsible for recruiting acetyltransferases including CBP/p300 and p/CAF for chromatin remodeling (Voegel et al., 1996; Li et al., 1997; Onate et al., 1998). The second transcriptional activation domain (AD2) is located at the C-terminus and is responsible for the interaction with the histone methyltransferases CARM1 and PRMT1 (Chen et al., 1999; Koh et al., 2001). In addition, *NCOA1* and *NCOA3* possess weak intrinsic HAT activities at the C-terminal region (Chen et al., 1997; Spencer et al., 1997). Moreover, *NCOA* proteins contain specific LXXLL motifs (where L is leucine and X is any amino acid), which arrange the interaction with nuclear receptors via the NID (three motifs), as well as with p300/CBP through the CID/AD1 (two motifs) (Heery et al., 1997; Kalkhoven et al., 1998). Importantly, the *NCOA* proteins are capable of interacting with multiple nuclear receptors in a ligand-dependent mode and significantly augment nuclear receptor-dependent transcriptional activity (Leo et al., 2000; McKenna and O'Malley, 2002; Xu and Li, 2003).

The structure and function of *PAX3* have been well reviewed (Buckingham and Relaix, 2007; Mercado and Barr, 2007). This member of the family of paired box transcription factors contains an N-terminal DNA-binding domain, a complete homeodomain and a proline- serine- and threonine-rich transcriptional activation domain. The *PAX3-NCOA1* and *PAX3-NCOA2* fusion genes produce mRNAs containing the 5' end of *PAX3* appended in translational frame to the 3' end of *NCOA1* or *NCOA2*. Similar to *PAX-FOXO1* fusion products, *PAX3-NCOA* fusion products retain the DNA binding domain of *PAX3*. The CBP/p300 interaction domain, the Q-rich region and AD2 transcriptional activation domain of the nuclear receptor coactivator proteins are also retained within the *PAX3-NCOA* chimeric products. In addition, the transactivation capability of the *PAX3-NCOA1* fusion protein using a luciferase reporter gene system appears to be comparable to *PAX3-FOXO1* (Wachtel et al., 2004).

In contrast, the *PAX3-NCOA* fusions do not retain the PAS/bNLH domain of the nuclear receptor coactivator protein, believed to be involved in DNA-binding and protein heterodimerization, or the receptor interacting domain (RID), which mediates the binding of transcriptional coactivators to nuclear receptors via conserved LXXLL/LXXLL motifs. Therefore, it is unlikely that *PAX3-NCOA1* or *-NCOA2* fusion proteins are able to interact with any of the upstream components that normally require *NCOA1* or *NCOA2* as a



transcriptional intermediary. Instead, the activity of AD1/CID may directly modulate or augment the transcriptional activity of genes normally regulated by PAX3 through recruiting CBP/p300. Alternatively, the intrinsic HAT and histone methyltransferase activities of the nuclear receptor coactivator moiety of the fusion oncogenes are relevant to putative sarcomagenic alterations in gene expression.

*NCOA2* and *NCOA3* have been identified in translocation events in other neoplastic entities. The C-terminal portion of *NCOA2* retained in the MYST3-*NCOA2* fusion protein generated by an inv(8)(p11q13) in acute myelogenous leukemia (AML) (Murati et al., 2004; Carapeti et al., 1998; Liang et al., 1998) and in the ETV6-*NCOA2* chimeric protein created by the t(8;12)(q13;p13) in pediatric acute lymphoblastic leukemia (Strehl et al., 2008) is identical to that preserved in the PAX3-*NCOA2* fusion. Fusion of the C-terminal portion of *NCOA3* to MYST3 has also been observed in an M5-AML (Esteyries et al., 2008). The involvement of the same functional domains of the nuclear receptor coactivators in various oncogenic fusion proteins emphasizes the importance of the CID/AD1 and AD2 regions in tumorigenesis. Fusion between *NCOA1* and genes other than *PAX3* has not been observed yet.

As demonstrated, a deletion in the CID/AD1 domain of *NCOA1* or *NCOA2* abrogated soft agar cloning. These data indicate that the conserved LXXLL motifs in CID/AD1 of *NCOA1* and *NCOA2* play a pivotal role in *PAX3-NCOA1* or *PAX3-NCOA2* mediated transformation. The activity of *NCOA1* and *NCOA2* is stimulated through recruiting CBP/p300 (Kim et al., 2001; Wang et al., 2001). CBP/p300 are universal transcription coactivators with HAT activity (Bannister and Kouzarides, 1996; Ogryzko et al., 1996;) that participate in multiple transcriptional events through the regulation of histone acetylation and interaction with the basal transcriptional machinery (Avantaggiati et al., 1997; von Mikecz et al., 2000;). CBP/p300 also contributes to the acetylation of non-histone proteins, such as RB1, E2F, and TP53 and regulates cell growth and differentiation. In the *PAX3-NCOA1* and *PAX3-NCOA2* fusions, CID, a CBP interacting domain in the nuclear receptor coactivator portion, is retained. This domain is required for NIH3T3 cells to form colonies in soft agar. In contrast, the deletion of AD2 from *NCOA1* and *NCOA2* produced only a fifty percent reduction in the number of soft agar colonies.

In conclusion, these data suggest that the nuclear receptor coactivator portion of the PAX3-*NCOA1* or -*NCOA2* fusion proteins is necessary to activate the oncogenic potential of PAX3 by providing activation domains for stimulating transcription or HAT activity for remodeling chromatin. The *PAX3* DNA-binding domains could deliver the CBP interaction domain (AD1) and histone methyltransferase domain (AD2) to unique chromosomal locations modifying transcription by allowing binding of CBP or other proteins and/or through remodeling the chromatin around the *PAX3* binding site. Additional studies will be needed to determine if the downstream genes and pathways activated by PAX3-*NCOA* fusions are shared or contrast with those stimulated by PAX-FOXO1 fusions. The discovery of these recurrent, novel translocations and associated fusion oncoproteins should shed light on the relationship between the control of chromatin condensation and gene expression in RMS and may further contribute to directed subtype-specific therapeutics.

## Acknowledgments

The authors would like to thank Dr. Beat Schäfer (University Children's Hospital, Zurich, Switzerland) for kindly providing a *PAX3-NCOA1* positive RNA control sample. The authors would also like to thank Dr. Gregorio Chejfec (University of Illinois Medical Center, Chicago, IL) and Dr. Diana Corao (DuPont Hospital for Children, Wilmington, DE) for their case material contributions.

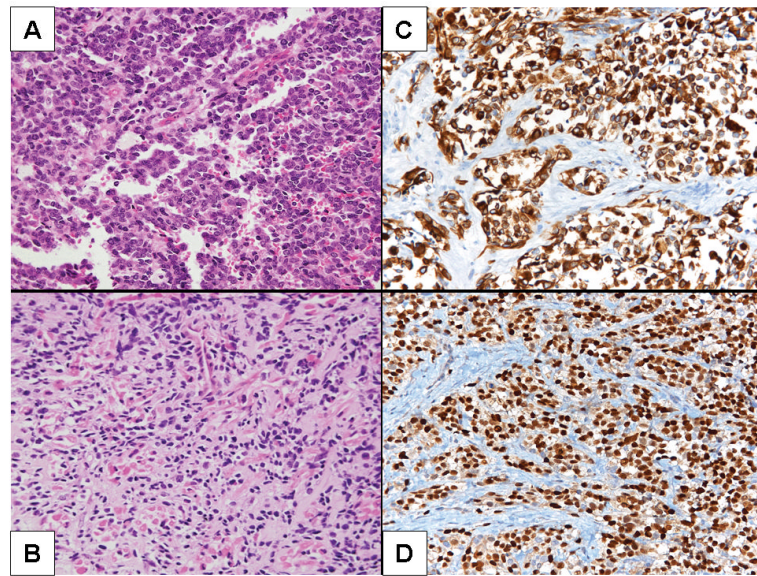
Supported by: This work was supported in part by the following: NIH U-10-CA98543-01, NIH RO1-CA89461, UNMC Eppley Pediatric Cancer Award, The Ohio division of the American Cancer Society, and the La Fondation des Gouverneurs de l'Espoir.

## References

- Avantaggiati ML, Ogryzko V, Gardner K, Giordano A, Levine AS, Kelly K. Recruitment of p300/CBP in p53-dependent signal pathways. *Cell*. 1997; 89:1175–1184. [PubMed: 9215639]
- Bannister AJ, Kouzarides T. The CBP co-activator is a histone acetyltransferase. *Nature*. 1996; 384:641–643. [PubMed: 8967953]
- Barr FG, Qualman SJ, Macris MH, Melnyk N, Lawlor ER, Strzelecki DM, Triche TJ, Bridge JA, Sorensen PH. Genetic heterogeneity in the alveolar rhabdomyosarcoma subset without typical gene fusions. *Cancer Res*. 2002; 62:4704–4710. [PubMed: 12183429]
- Bridge JA, Liu J, Weibolt V, Baker KS, Perry D, Kruger R, Qualman S, Barr F, Sorensen P, Triche T, Suijkerbuijk R. Novel genomic imbalances in embryonal rhabdomyosarcoma revealed by comparative genomic hybridization and fluorescence in situ hybridization: an intergroup rhabdomyosarcoma study. *Genes Chromosomes Cancer*. 2000; 27:337–344. [PubMed: 10719362]
- Buckingham M, Relaix F. The role of Pax genes in the development of tissues and organs: Pax3 and Pax7 regulate muscle progenitor cell functions. *Annual Rev Cell Dev Biol*. 2007; 23:645–673. [PubMed: 17506689]
- Carapeti M, Aguiar RC, Goldman JM, Cross NC. A novel fusion between MOZ and the nuclear receptor coactivator TIF2 in acute myeloid leukemia. *Blood*. 1998; 91:3127–3133. [PubMed: 9558366]
- Carr PA, Park JS, Lee YJ, Yu T, Zhang S, Jacobson JM. Protein-mediated error correction for de novo DNA synthesis. *Nucleic Acids Res*. 2004; 32:e162. [PubMed: 15561997]
- Chen H, Lin RJ, Schiltz RL, Chakravarti D, Nash A, Nagy L, Privalsky ML, Nakatani Y, Evans RM. Nuclear receptor coactivator ACTR is a novel histone acetyltransferase and forms a multimeric activation complex with P/CAF and CBP/p300. *Cell*. 1997; 90:569–580. [PubMed: 9267036]
- Chen D, Ma H, Hong H, Koh SS, Huang SM, Schurter BT, Aswad DW, Stallcup MR. Regulation of transcription by a protein methyltransferase. *Science*. 1999; 284:2174–2177. [PubMed: 10381882]
- Davicioni E, Anderson MJ, Finckenstein FG, Lynch JC, Qualman SJ, Shimada H, Schofield DE, Buckley JD, Meyer WH, Sorensen PH, Triche TJ. Molecular classification of rhabdomyosarcoma--genotypic and phenotypic determinants of diagnosis: a report from the Children's Oncology Group. *Am J Pathol*. 2009; 174:550–564. [PubMed: 19147825]
- Davis RJ, D'Cruz CM, Lovell MA, Biegel JA, Barr FG. Fusion of PAX7 to FKHR by the variant t(1;13)(p36;q14) translocation in alveolar rhabdomyosarcoma. *Cancer Res*. 1994; 54:2869–2872. [PubMed: 8187070]
- Deguchi K, Ayton PM, Carapeti M, Kutok JL, Snyder CS, Williams IR, Cross NC, Glass CK, Cleary ML, Gilliland DG. MOZ-TIF2-induced acute myeloid leukemia requires the MOZ nucleosome binding motif and TIF2-mediated recruitment of CBP. *Cancer Cell*. 2003; 3:259–271. [PubMed: 12676584]
- Esteyries S, Perot C, Adelaide J, Imbert M, Lagarde A, Pautas C, Olschwang S, Birnbaum D, Chaffanet M, Mozziconacci MJ. NCOA3, a new fusion partner for MOZ/MYST3 in M5 acute myeloid leukemia. *Leukemia*. 2008; 22:663–665. [PubMed: 17805331]
- Galili N, Davis RJ, Fredericks WJ, Mukhopadhyay S, Rauscher FJ, Emanuel BS, Rovera G, Barr FG. Fusion of a fork head domain gene to PAX3 in the solid tumour alveolar rhabdomyosarcoma. *Nat Genet*. 1993; 3:230–235. [PubMed: 8275086]
- Hayashi Y, Inaba T, Hanada R, Yamamoto K. Translocation 2;8 in a congenital rhabdomyosarcoma. *Cancer Genet Cytogenet*. 1988; 30:343–345. [PubMed: 3342389]
- Heery DM, Kalkhoven E, Hoare S, Parker MG. A signature motif in transcriptional co-activators mediates binding to nuclear receptors. *Nature*. 1997; 387:733–736. [PubMed: 9192902]
- Kalkhoven E, Valentine JE, Heery DM, Parker MG. Isoforms of steroid receptor co-activator 1 differ in their ability to potentiate transcription by the oestrogen receptor. *EMBO J*. 1998; 17:232–243. [PubMed: 9427757]

- Kapels KM, Nishio J, Zhou M, Qualman SJ, Bridge JA. Embryonal rhabdomyosarcoma with a der(16)t(1;16) translocation. *Cancer Genet Cytogenet.* 2007; 174:68–73. [PubMed: 17350470]
- Kim MY, Hsiao SJ, Kraus WL. A role for coactivators and histone acetylation in estrogen receptor alpha-mediated transcription initiation. *EMBO J.* 2001; 20:6084–6094. [PubMed: 11689448]
- Koh SS, Chen D, Lee YH, Stallcup MR. Synergistic enhancement of nuclear receptor function by p160 coactivators and two coactivators with protein methyltransferase activities. *J Biol Chem.* 2001; 276:1089–1098. [PubMed: 11050077]
- Leo C, Chen JD. The SRC family of nuclear receptor coactivators. *Gene.* 2000; 245:1–11. [PubMed: 10713439]
- Li S, Aufiero B, Schiltz RL, Walsh MJ. Regulation of the homeodomain CCAAT displacement/cut protein function by histone acetyltransferases p300/CREB-binding protein (CBP)-associated factor and CBP. *Proc Natl Acad Sci USA.* 2000; 97:7166–7171. [PubMed: 10852958]
- Liang J, Prouty L, Williams BJ, Dayton MA, Blanchard KL. Acute mixed lineage leukemia with an inv(8)(p11q13) resulting in fusion of the genes for MOZ and TIF2. *Blood.* 1998; 92:2118–2122. [PubMed: 9731070]
- Lugo TG, Witte ON. The BCR-ABL oncogene transforms Rat-1 cells and cooperates with v-myc. *Mol Cell Biol.* 1989; 9:1263–1270. [PubMed: 2725497]
- McKenna NJ, O'Malley BW. Minireview: nuclear receptor coactivators, an update. *Endocrinology.* 2002; 143:2461–2465. [PubMed: 12072374]
- Meloni-Ehrig A, Smith B, Zgoda J, Greenberg J, Perdahl-Wallace E, Zaman S, Mowrey P. Translocation (2;8)(q35;q13): a recurrent abnormality in congenital embryonal rhabdomyosarcoma. *Cancer Genet Cytogenet.* 2009; 191:43–45. [PubMed: 19389508]
- Mercado GE, Barr FG. Fusions involving PAX and FOX genes in the molecular pathogenesis of alveolar rhabdomyosarcoma: recent advances. *Curr Mol Med.* 2007; 7:47–61. [PubMed: 17311532]
- von Mikecz A, Zhang S, Montminy M, Tan EM, Hemmerich P. CREB-binding protein (CBP)/p300 and RNA polymerase II colocalize in transcriptionally active domains in the nucleus. *J Cell Biol.* 2000; 150:265–273. [PubMed: 10893273]
- Murati A, Adélaïde J, Mozziconacci MJ, Popovici C, Carbuccia N, Letessier A, Birg F, Birnbaum D, Chaffanet M. Variant MYST4-CBP gene fusion in a t(10;16) acute myeloid leukaemia. *Br J Haematol.* 2004; 125:601–604. [PubMed: 15147375]
- Nishio J, Althof PA, Bailey JM, Zhou M, Neff JR, Barr FG, Parham DM, Teot L, Qualman SJ, Bridge JA. Use of a novel FISH assay on paraffin-embedded tissues as an adjunct to diagnosis of alveolar rhabdomyosarcoma. *Lab Invest.* 2006; 86:547–556. [PubMed: 16607381]
- Ogryzko VV, Schiltz RL, Russanova V, Howard BH, Nakatani Y. The transcriptional coactivators p300 and CBP are histone acetyltransferases. *Cell.* 1996; 87:953–959. [PubMed: 8945521]
- Onate SA, Boonyaratanakornkit V, Spencer TE, Tsai SY, Tsai MJ, Edwards DP, O'Malley BW. The steroid receptor coactivator-1 contains multiple receptor interacting and activation domains that cooperatively enhance the activation function 1 (AF1) and AF2 domains of steroid receptors. *J Biol Chem.* 1998; 273:12101–12108. [PubMed: 9575154]
- Parham DM, Ellison DA. Rhabdomyosarcomas in adults and children: an update. *Arch Pathol Lab Med.* 2006; 130:1454–1465. [PubMed: 17090187]
- Polito P, Dal Cin P, Sciort R, Brock P, Van Eykan P, Van Den Berghe H. Embryonal rhabdomyosarcoma with only numerical chromosome changes. Case report and review of the literature. *Cancer Genet Cytogenet.* 1999; 109:161–165. [PubMed: 10087953]
- Qualman SJ, Coffin CM, Newton WA, Hojo H, Triche TJ, Parham DM, Crist WM. Intergroup Rhabdomyosarcoma study: Update for pathologists. *Pediatr Dev Pathol.* 1998; 1:550–561. [PubMed: 9724344]
- Raney RB, Anderson JR, Barr FG, Donaldson SS, Pappo AS, Qualman SJ, Wiener ES, Maurer HM, Crist WM. Rhabdomyosarcoma and undifferentiated sarcoma in the first two decades of life: a selective review of intergroup rhabdomyosarcoma study group experience and rationale for Intergroup Rhabdomyosarcoma Study V. *J Pediatr Hematol Oncol.* 2001; 23:215–220. [PubMed: 11846299]

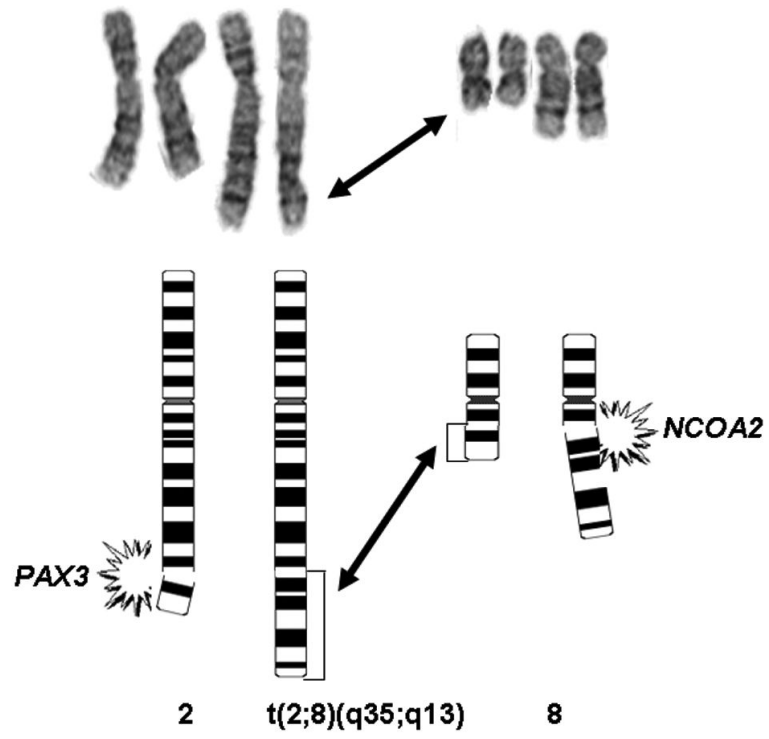
- Shaffer, LG.; Slovak, ML.; Campbell, LJ., editors. An International System for Human Cytogenetic Nomenclature Basel. Karger, ISCN; 2009.
- Sorensen PH, Lynch JC, Qualman SJ, Tirabosco R, Lim JF, Maurer HM, Bridge JA, Crist WM, Triche TJ, Barr FG. PAX3-FKHR and PAX7-FKHR gene fusions are prognostic indicators in alveolar rhabdomyosarcoma: a report from the children's oncology group. *J Clin Oncol.* 2002; 11:2672–2679. [PubMed: 12039929]
- Spencer TE, Jenster G, Burcin MM, Allis CD, Zhou J, Mizzen CA, McKenna NJ, Onate SA, Tsai SY, Tsai MJ, O'Malley BW. Steroid receptor coactivator-1 is a histone acetyltransferase. *Nature.* 1997; 389:194–198. [PubMed: 9296499]
- Strehl S, Nebral K, König M, Harbott J, Strobl H, Rätei R, Struski S, Bielorai B, Lessard M, Zimmermann M, Haas OA, Izraeli S. ETV6-NCOA2: a novel fusion gene in acute leukemia associated with coexpression of T-lymphoid and myeloid markers and frequent NOTCH1 mutations. *Clin Cancer Res.* 2008; 14:977–983. [PubMed: 18281529]
- Torchia J, Rose DW, Inostroza J, Kamei Y, Westin S, Glass CK, Rosenfeld MG. The transcriptional co-activator p/CIP binds CBP and mediates nuclear-receptor function. *Nature.* 1997; 387:677–684. [PubMed: 9192892]
- Voegel JJ, Heine MJ, Zechel C, Chambon P, Gronemeyer H. TIF2, a 160 kDa transcriptional mediator for the ligand-dependent activation function AF-2 of nuclear receptors. *EMBO J.* 1996; 15:3667–3675. [PubMed: 8670870]
- Wachtel M, Dettling M, Koscielniak E, Stegmaier S, Treuner J, Simon-Klingenstein K, Bühlmann P, Niggli FK, Schäfer BW. Gene expression signatures identify rhabdomyosarcoma subtypes and detect a novel t(2;2)(q35;p23) translocation fusing PAX3 to NCOA1. *Cancer Res.* 2004; 64:5539–5545. [PubMed: 15313887]
- Wang C, Fu M, Angeletti RH, Siconolfi-Baez L, Reutens AT, Albanese C, Lisanti MP, Katzenellenbogen BS, Kato S, Hopp T, Fuqua SA, Lopez GN, Kushner PJ, Pestell RG. Direct acetylation of the estrogen receptor alpha hinge region by p300 regulates transactivation and hormone sensitivity. *J Biol Chem.* 2001; 276:18375–18383. [PubMed: 11279135]
- Yoshino K, Takeuchi M, Nakayama M, Suehara N. Congenital cervical rhabdomyosarcoma arising in one fetus of a twin pregnancy. *Fetal Diagn Ther.* 2005; 20:291–295. [PubMed: 15980643]
- Xu J, Li Q. Review of the in vivo functions of the p160 steroid receptor coactivator family. *Mol Endocrinol.* 2003; 17:1681–1692. [PubMed: 12805412]
- Xu J, O'Malley BW. Molecular mechanisms and cellular biology of the steroid receptor coactivator (SRC) family in steroid receptor function. *Rev Endocr Metab Disord.* 2002; 3:185–192. [PubMed: 12215713]
- Zhuravleva J, Paggetti J, Martin L, Hammann A, Solary E, Bastie JN, Delva L. MOZ/TIF2-induced acute myeloid leukaemia in transgenic fish. *Br J Haematol.* 2008; 143:378–382. [PubMed: 18729850]



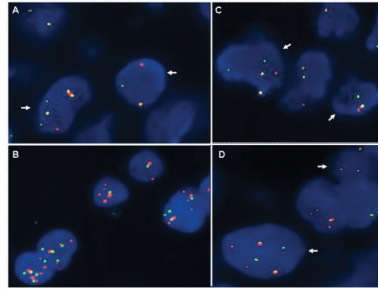
**Figure 1.**

**A.** Alveolar rhabdomyosarcoma, Case 1. Note the loss of cellular cohesion. **B.** Scattered rhabdomyoblasts with eosinophilic cytoplasm in Case 5, embryonal rhabdomyosarcoma. **C and D.** Case 4, desmin and myogenin immunoreactivity, respectively.





**Figure 2.**  
 Partial karyotype and schematic illustrating the t(2;8)(q35;q12) identified in Case 4.

**Figure 3.**

Representative FISH analysis of t(2;2)(p23;q35) and t(2;8)(q35;q12) translocations. **A.** FISH analysis of Case 1 with the custom designed *NCOA1* break-apart probe set demonstrates split orange and green signals (arrows) indicative of a rearrangement of this locus. **B.** FISH analysis of Case 1 with the *PAX3* spanning probe set in orange and the *NCOA1* spanning probe set in green demonstrates the presence of juxtaposed or fused orange and green signals consistent with the RT-PCR findings of a *PAX3-NCOA1* fusion transcript in this case. **C and D.** FISH analyses of Case 4 with the custom designed *PAX3* and *NCOA2* break-apart probe sets, respectively, demonstrate split orange and green signals (arrows) indicative of a rearrangement of each of these loci.

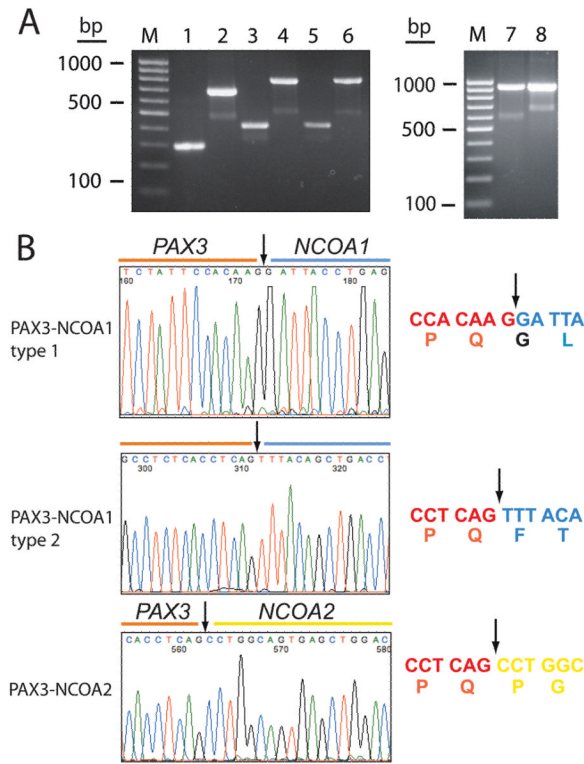


**Figure 4.** Representative RT-PCR and sequence analyses for chimeric transcripts in Cases 1-5. **A.** Detection of *PAX3-NCOA1* transcripts in Case 1 (lanes 1 and 2); 2 (lanes 3 and 4) and 3 (lanes 5 and 6). Primers used for lanes 1, 3 and 5 were PAX3-32 and NCOA1-33; for lanes 2, 4 and 6, PAX3-34 and NCOA1-35. Detection of *PAX3-NCOA2* transcripts in Cases 4 (lane 7) and 5 (lane 8). Primers used were PAX3-41 and NCOA2-48. **B.** Sequence alignment of the *PAX3-NCOA1* and *PAX3-NCOA2* breakpoint regions. Arrows depict the fusion point. Single letter amino acid code is displayed beneath the nucleotide sequence.



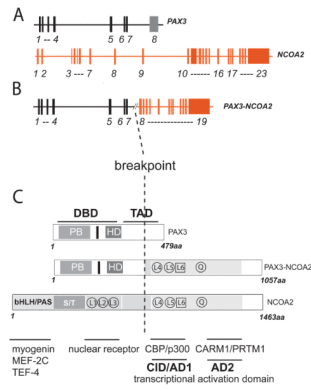


**Figure 6.**  
**A and B.** Genomic structure of *PAX3*, *NCOA2* and the *PAX3-NCOA2* fusion (*PAX3* exons 1-7 and *NCOA2* exons 12-23). **C.** *PAX3*, *NCOA2* and *PAX3-NCOA2* proteins. Refer to Figure 4D legend for structure description.



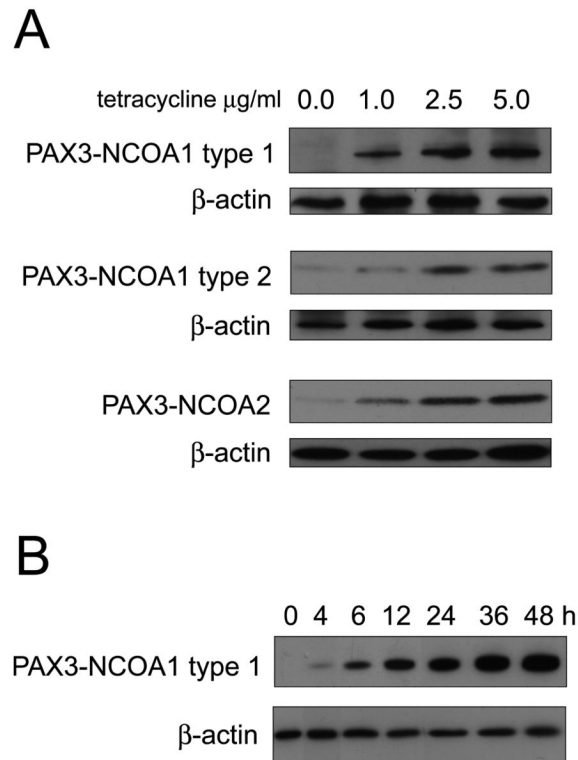


**Figure 7.**

Tetracycline inducible expression of *PAX3-NCOA1* and *PAX3-NCOA2* genes in transfected NIH 3T3 cells. **A.** Representative Western blots demonstrate the induction of varying expression levels of *PAX3-NCOA1* type 1, *PAX3-NCOA1* type 2 and *PAX3-NCOA2* chimeric genes that correspond with different doses of tetracycline. **B.** Western blot demonstrating the rapid induction of *PAX3-NCOA1* type 1 expression in the presence of 2.5  $\mu\text{g/ml}$  tetracycline (cells were harvested at the time points indicated).

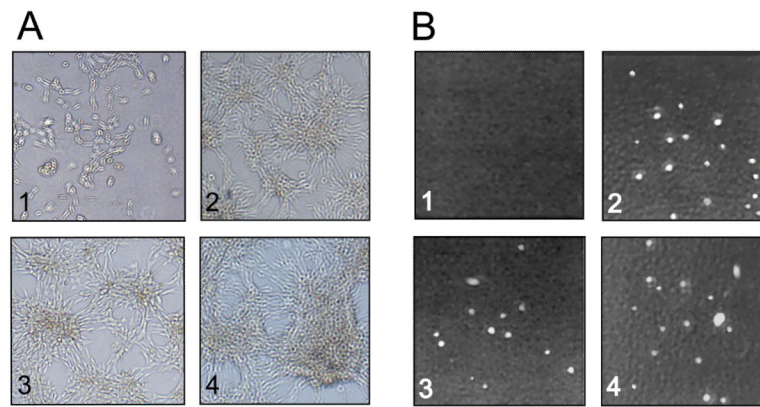


**Figure 8.**

Effect of PAX3-NCOA1 type 1, PAX3-NCOA1 type 2 and PAX3-NCOA2 expression on NIH3T3 cell growth. **A.** NIH3T3-Tet-19.1 cells transfected with plasmids pcDNA4/TO (1), PAX3-NCOA1-type 1 (2), PAX3-NCOA1-type 2 (3) and PAX3-NCOA2 (4) in pcDNA4/TO and grown in the presence of 1 µg/ml tetracycline. **B.** Representative agar assay images acquired 2 weeks after cells were plated at low density and grown in the presence of 1 µg/ml tetracycline show formation of macroscopic colonies in the PAX3-NCOA1-type 1 (2), PAX3-NCOA1-type 2 (3) and PAX3-NCOA2 (4) plates but not in the pcDNA4/TO (1) plate.

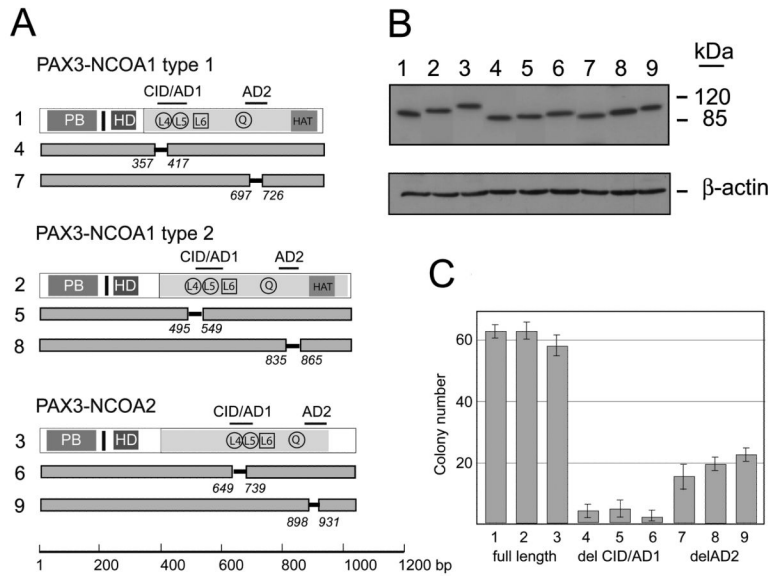


**Figure 9.** Analyses of transforming activities of PAX3-NCOA1 and PAX3-NCOA2 fusion proteins and deletion mutants. **A.** Schematic structure of PAX3-NCOA1, PAX3-NCOA2 and deletion mutants. Solid bars with amino acid position displays the regions deleted. **B.** Immunoblot analyses of PAX3-NCOA1, PAX3-NCOA2 and deletion mutants in NIH3T3-Tet-19.1.E. **C.** Soft agar colony assay of pcDNA4/TO vector (1), pcDNA4/TO-PAX3-NCOA1 type 1, pcDNA4/TO-PAX3-NCOA1 type 2, and pcDNA4/TO-PAX3-NCOA2 transduced NIH3T3-Tet-19.1 cells. Cells were incubated in the presence of 1 $\mu$ g/ml tetracycline and scored after 14 days. Three plates were counted for each construct.

Table 1

Clinicopathologic, Cytogenetic, and Fusion Gene Data

Case	Age <sup>d</sup> / Sex	Location <sup>b</sup> (size in cm)	Histopathologic Diagnosis <sup>c</sup>	Karyotype <sup>d</sup>	Fusion Gene <sup>e</sup>
1	22/M	Base of skull (2.0 × 1.3 × 1.1)	ARMS	NP	PAX3- <i>NGOAI</i>
2	5/M	Gluteus maximus N/A	ARMS	46,XY[15]	PAX3- <i>NGOAI</i>
3	18/F	Perineum N/A	ARMS	NP	PAX3- <i>NGOAI</i>
4	2/M	Testis (5.0 × 2.5 × 2.3)	ARMS	66-90,XY,add(X)(p11)×2, t(2;8)(q35;q12)×2[cp12]/46,XY[3]	PAX3- <i>NGOAI</i>
5	2wk/ M	Perineum (3.7 × 4.1 × 3.2)	ERMS	46,XY,t(2;8)(q35;q13)[6]/46,XY[14] <sup>f</sup>	PAX3- <i>NGOAI</i>

<sup>a</sup> Age is in years unless otherwise stated<sup>b</sup> All cases were primary lesions<sup>c</sup> ARMS, alveolar rhabdomyosarcoma; ERMS, embryonal rhabdomyosarcoma<sup>d</sup> N/A, not available; NP, not performed<sup>e</sup> Fusion gene status for each case as confirmed by FISH and RT-PCR with subsequent sequencing<sup>f</sup> This karyotype has been reported previously (Meloni-Ehrig et al., 2009)

**Table 2**Optimized *NCOA1* and *NCOA2* FISH Probe Sets

Probe set	Clone <sup>a</sup>	Location	Label
RP11-715M22	BAC	Proximal to <i>NCOA1</i> locus	Spectrum green
RP11-24J3	BAC	Distal to <i>NCOA1</i> locus	Spectrum orange
RP11-1109B14/RP11-803B18	BAC cocktail	Spans <i>NCOA1</i> locus	Spectrum green
CTD-2606A20/RP11-68N15	BAC cocktail	Proximal to <i>NCOA2</i> locus	Spectrum green
RP11-680D10/RP11-133E24	BAC cocktail	Distal to <i>NCOA2</i> locus	Spectrum orange
RP11-479K21/RP11-183D21	BAC cocktail	Spans <i>NCOA2</i> locus	Spectrum green

<sup>a</sup>BAC, bacterial artificial chromosome



**Table 3**

Oligonucleotides Used in RACE and RT-PCR Studies

Gene	Sequence	Position of the Primer <sup>1</sup>
PAX3-32	GCTTTCAACCTCTCTTCCCG	exon 6; 853-874 n
PAX3-34	CCAGCCCACATCTATTCCACAAG	exon 7; 936-958 n
NCOA1-33	TAATACATCTAATCCACCCCCTG	exons 13-14; 2883-2906 n
NCOA1-35	GCCTTCTCATCATTTCTCCCTTCTACTG	exon 13; 2764-2792 n
NCOA1-40; RACE	CCATCCTGTCTGTCTCACATAAGCC	exon 13; 2743-2767 n
PAX3-41	TGGAGCGTGCTTTTGAGAGAAC	exon 5; 701-722 n
PAX3-43	TCCTTCCAACCCAGACAGCAG	exon 7; 1032-1052 n
PAX3-45; RACE	CTGCCTCCCCAGCACCAG	exon 7; 1062-1079 n
PAX3-47; RACE	GCTTTCAACCATCTCATTCCCG	exon 6; 864-874 n
PAX3-42; RACE	ATGGCAGTGGGAGGGAACC	exon 7; 1244-1263 n
NCOA2-44	CGGTGCCCATTTCTCCAGATG	exon 13; 3011-3030 n
NCOA2-46; RACE	GCAGTGCTGTTTTCTGGGCTC	exon 12; 2732-2752 n
NCOA2-48	TCTCACAGCCGA ACTCTGCG	exon 13; 3029-3048 n

<sup>1</sup>Position in the wild type *PAX3* (NM\_181457), *NCOA1* (NM\_003743) and *NCOA2* (NM\_006540) genes; n = nucleotide position.

**Table 4**Oligonucleotides Used in the Construction of *PAX3-NCOA1* and *PAX3-NCOA2* Deletion Mutants

Gene	Primer	Sequence
	AD1-PN1.1-357u	GCTATAAATCAGAGTAAATCAGCTCTTGAACAGCTGGTATCC'
	AD1-PN1.1-357l	GGATACCAGCTGTTCAAGAGCTGATTTACTCTGATTTATAGC
<i>PAX3-NCOA1</i> type 1	AD1-PN1.1-417u	GCTATAAATCAGAGTAAATCGGTGGATTAGATGTATTATCAGAG
	AD1-PN1.1-417l	CTCTGATAATACATCTAATCCACCGATTTACTCTGATTTATAGC
	AD2-PN1.1-697-727u	GTTCCCAAGGTGAGGCCAACGCCTCCGGGTATCAGACATGA
	AD2-PN1.1-697-727l	TCATGTCTGATACCCGGAGGCGTTGGCCTCACCTTGGGGAAC
	AD1-PN1.2-495u	GAAGACCAGTGTATTAGCGAGAAGGCTTCTTCTTGA
	AD1-PN1.2-495l	TCAAGAAGAAGCCTTCTCGCTAATACTACTGGTCTTC
<i>PAX3-NCOA1</i> type 2	AD1-PN1.2-549u	GAAGACCAGTGTATTAGCGGTGGATTAGATGTATTAATCAG
	AD1-PN1.2-549l	CTGATTAATACATCTAATCCACCGCTAATACTACTGGTCTTC
	AD2-PN1.2-835-865u	GGTGAGGCCAACTTIGCTCCATCTCTAGACATGAAGGCCTGGCAGCAA
	AD2-PN1.2-835-865l	TTGCTGCCAGGCCTTCATGTCTAGAGATGGAGCAAAGTTGGCCTCACC
	AD1-PN2-649u	GCCAGCCAAAACAGGCAGCCAGACCAGGTGTATCTGGCCTTGCGG
	AD1-PN2-649l	CCGCAAGGCCAGATACACCTGGTCTGGCTGCCTGTTTTGGCTGGC
<i>PAX3-NCOA2</i>	AD1-PN2-739u	GCCAGCCAAAACAGGCAGCCAGACCAGGTAGCTATTGCCCCATGCAAGATCCA
	AD1-PN2-739l	TGGATCTTGCATGGGCGAATAGCTACCTGGTCTGGCTGCCTGTTTTGGCTGGC
	AD2- PN2-898-93u	CAGCAGTTTCCATTTCTCCTCAAACCTACCCAACAGTCTCAGGCCAACCCAGCC
	AD2- PN2-898-93l	GGCTGGGTTGGCCTGAGACTGTTGGGTAGTTTTGGAGGAAATGGAAACTGCTG

u= upper strand primer; l=lower strand primer